Comparison of Melted Corium Relocation during Severe Accident of High Temperature Reactor using Moving Particle Semi-Implicit Method

Muhamad Irfan[1,a], Ismail Humolungo[1], Asril Pramutadi Andi Mustari[1,2], Sidik Permana[1,2]

[1]Department of Nuclear Science and Engineering, Institut Teknologi Bandung, Indonesia

[2]Department of Physics, Institut Teknologi Bandung, Indonesia

[a]irfan_aldrs@yahoo.com

Abstract. *System failure in nuclear reactors can cause degradation of a reactor core, allowing melting and relocation of the corium to the lower plenum in the nuclear reactor system. In this study, a severe accident simulation was carried out using the Moving Particle Semi-Implicit (MPS) method. In this method, we model the relocation of molten corium on the reactor core (support plate) to the lower plenum for several conditions with variations: corium material, lower plenum conditions, temperature, viscosity, and density. Those treatments were performed in order to be able to compare and analyze the characteristics of the corium melt by reviewing the velocity profiles. The formation of a corium pool and debris bed can result in significant temperature differences and high heat flux against the walls of the reactor vessel, causing a decrease in the integrity of the reactor vessel and reactor failure.*

Keywords: Corium, uranium dioxide (UO_2), zirconium dioxide (ZrO_2), fluid relocation, moving particle semi-implicit (MPS).

Introduction

The occurrence of system failure in nuclear reactors can lead to the deterioration of the reactor core, resulting in the melting and relocation of the corium towards the lower plenum within the nuclear reactor system. This greatly determines the level of damage to the core and reactor vessel which impact to the release of radioactive particles into the environment [1]. This kind of situation can be simulated by carrying out a simple approach and modeling of the reactor geometry and molten corium relocation with the semi-implicit moving particle (MPS) method as the first step in analyzing the characteristics of corium melt relocation to prevent and predict the level of damage to the core and reactor vessel [2]. The MPS method was developed since 1996 by S. Koshizuka and K.Shibata from Waseda University, Japan, who developed a meshless particle method to analyze incompressible flows so that numerical stability and computational speed increased significantly.

In this study a severe accident simulation was carried out on the high temperature nuclear reactor using the MPS method by modeling the relocation of molten corium from the reactor core (support plate) to the lower plenum for several conditions with variations in corium material, lower plenum conditions, temperature, viscosity, and density in order to perform comparisons and analyze the

characteristics of the corium melt by reviewing the velocity profiles in these various conditions, as well as their graphs against time.

This research was carried out with five variations of corium material with different compositions of UO_2 and ZrO_2. Corium is a mixture of UO_2 and ZrO_2 as the most abundant material in the reactor core. Then, three variations were made on the condition of the lower plenum which is empty, filled with fluid, and filled with debris. The MPS used is only able to model one type of fluid so that the fluid in the lower plenum is the same fluid as the fluid material being relocated. Furthermore, three temperature variations were carried out with the temperature conditions used being the temperature between the melting point and boiling point of the material because the material is in the liquid phase. Viscosity and density variations follow temperature variations because viscosity and density are functions of temperature. The geometry of the reactor is simplified and scaled down.

Theoretical Background

The MPS method is a numerical method that has significantly increased stability and computational speed which is used for modeling incompressible fluid fragmentation. The equation for incompressible flow that is commonly used mathematically can be shown in the following equation [3],

$$\frac{\partial \rho}{\partial t} = 0 \tag{1}$$

$$\frac{\partial u}{\partial t} = -\frac{1}{\rho}\nabla P + v\Delta^2 u + g \tag{2}$$

$$\frac{\partial h}{\partial t} = k\nabla^2 T + Q \tag{3}$$

With $\rho, u, P, v, g, h, k, T$ and Q denote density, velocity, pressure, kinematic viscosity, gravity, enthalpy, thermal conductivity, temperature and heat source. Equation (1) states the conservation of mass, equation (2) states the Navier-Stokes equation which is affected by particle displacement, and equation (3) states the conservation of energy. The interaction between particles within the effective radius of each is considered in the MPS method. Mathematically, this interaction is shown in equation (4) below [3],

$$w(r) = \begin{cases} 1 - \frac{r}{r_e} & 0 \le r \le r_e \\ 0 & r_e \le r \end{cases} \tag{4}$$

With $w(r)$ expressing the weight function which represents the interaction between particles. The particle density which is the total weight function of the particles with $\vec{r_j}$ and $\vec{r_i}$ are the position vectors of particles i and j which is expressed in equation (5) below,

$$n_i = \sum_{j \ne i} w(|\vec{r_j} - \vec{r_i}|) \tag{5}$$

Particle interactions expressed in the gradient, divergence, and Laplacian operators are shown in equations (6), (7), and (8) as follows,

$$\langle \nabla \phi \rangle_i = \frac{d}{n^0} \sum_{j \neq i} \left[\frac{\phi_j - \widehat{\phi}_i}{|\vec{r_j} - \vec{r_i}|^2} (\vec{r_j} - \vec{r_i}) \omega \left(|\vec{r_j} - \vec{r_i}| \right) \right] \tag{6}$$

$$\langle \nabla \cdot u \rangle_i = \frac{d}{n^0} \sum_{j \neq i} \left[\frac{(\overline{u_j} - \overline{u_i}) \cdot (\vec{r_j} - \vec{r_i})}{|\vec{r_j} - \vec{r_i}|^2} \omega \left(|\vec{r_j} - \vec{r_i}| \right) \right] \tag{7}$$

$$\langle \nabla^2 \phi \rangle_i = \frac{d2}{\lambda n^0} \sum_{j \neq i} \left[(\phi_j - \phi_i) \omega \left(|\vec{r_j} - \vec{r_i}| \right) \right] \tag{8}$$

Where $d, n^0, \phi_j, \widehat{\phi}_i$ are the number of spatial dimensions, the density of the number of particles, the scalar value of particle j at $\vec{r_j}$ and the minimum scalar value of the target particle i. The value of λ is shown in equation (9) below,

$$\lambda = \frac{\sum_{j \neq i} w |\vec{r_j} - \vec{r_i}| (|\vec{r_j} - \vec{r_i}|)^2}{\sum_{j \neq i} w |\vec{r_j} - \vec{r_i}|} \cong \frac{\int w(r) r^2 dV}{\int w(r) dV} \tag{9}$$

The semi-implicit algorithm is used in the MPS method. MPS will implicitly calculate the pressure gradient, while viscosity, gravity, and temperature are calculated explicitly. The momentum equation will be calculated explicitly at each time so that the velocity and temporal position values of the particles are obtained, then the pressure is calculated implicitly by equation (10).

$$\langle \nabla^2 P \rangle^{k+1} = -\frac{\rho^0}{\Delta t^2} \frac{n^* - n^0}{n^0} \tag{10}$$

$$\vec{u}^{k+1} = \vec{u}^* - \frac{\Delta t}{\rho^0} \nabla P \tag{11}$$

$$\vec{r}^{k+1} = \vec{r}^* - \frac{\Delta t^2}{\rho^0} \nabla P \tag{12}$$

Equations (11) and (12) show the position and velocity of the particles with a pressure gradient [4].

The MPS method is widely used in various research fields, such as observing bubbly flows with complex interfaces using the multiphase MPS method. Then, in other studies the MPS method can also be used to review the effect of thrombus on the flow of red blood cells in the microvascular. In the nuclear field, the MPS method can be used as research conducted by Chen, R, et al., the MPS method is used to investigate numerically the behavior of frozen melt in a tube, taking into account surface tension and viscosity variations with temperature indicating that the crust formed on the surface the tube increases the resistance to flow of the melt, and will also slow down the solidification process of the melt. The melt penetration rate decreases significantly after the melt temperature drops to the melting point as a result of increasing the melt viscosity. In general, the results of this study indicate that the MPS method has the capacity to analyze the penetration behavior of melt in the instrument tube of the reactor vessel [5].

In addition, it can also be used to analyze the behavior of melt spread and molten corium concrete interaction (MCCI) as research conducted by Yamaji, A., and Li, X., which this phenomenon is important in the final phase of the accident for the assessment of containment integrity and

managing severe accidents. This MPS method can improve analytical skills and mechanical understanding of melt behavior in severe accident conditions. The MPS method has also been developed and verified with respect to radiation and thermal field calculations, solid-liquid phase transition, buoyancy, and viscosity-temperature dependence to simulate phenomena such as corium spreading, concrete ablation by corium, crust formation, and corium cooling by top flooding [4].

Methodology

In this study, parameter surveys were carried out by varying the lower plenum condition (empty lower plenum, fluid lower plenum, and debris lower plenum), material temperature (3500K, 4000K, and 4500K), and material (corium 1: 80% UO_2 & 20% ZrO_2, corium 2: 50% UO_2 & 50% ZrO_2, corium 3: 20% UO_2 & 80% ZrO_2, UO_2, and ZrO_2).

The condition variation scheme carried out in this study shown in Figure 1 below,
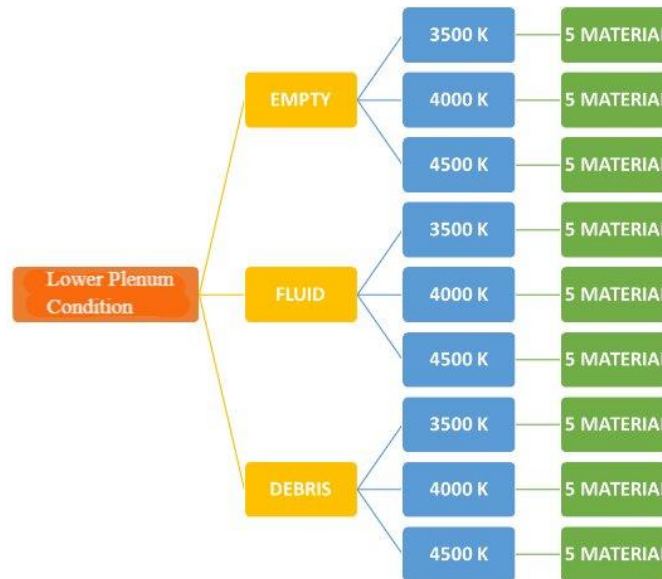
Figure 1.   Variation scheme in this study

The geometry of the reactor pressure vessel (RPV) built using the MPS method adapts to the geometry of general small modular reactor dimension of the high temperature reactor by simplifying and reducing the scale (scale-down) of the reactor geometry. Table 1 shows dimensions of the reactor geometry,

Table 1. The reactor dimensions

Dimension of Reactor Pressure Vessel (RPV)	
Inner Diameter of Support Plate (cm)	200
Thickness of Support Plate (cm)	20
Inner Diameter of Reactor Vessel (cm)	320
Thickness of Reactor Vessel (cm)	20
Distance from Support Plate to Lower Plenum (cm)	250

Figure 2 shows the simplification and scale-down of the RPV geometry built using the MPS method by distinguishing three types of particles: dummy wall particles (red), wall particles (yellow), and fluid particles (blue). Dummy wall particles are used to maintain geometric stability.

(a)   (b)   (c)
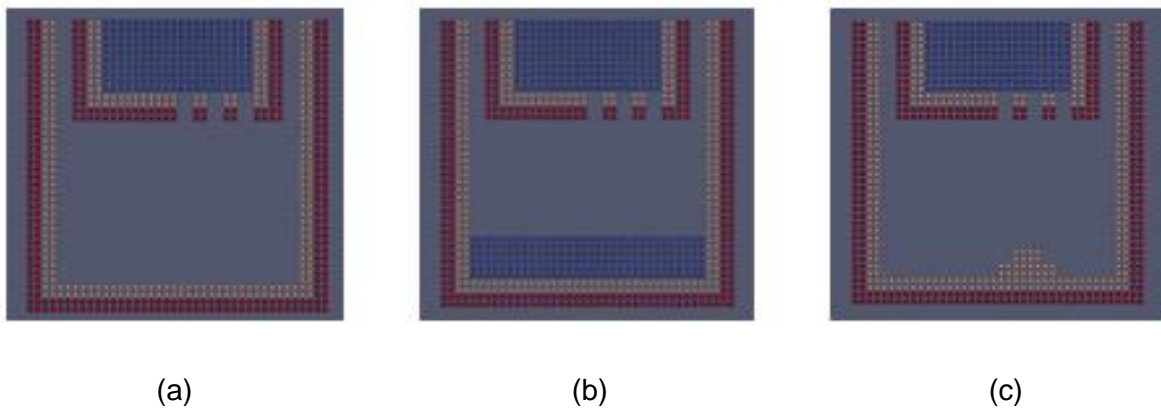
Figure 2.   The RPV geometry at MPS (a) Empty Lower Plenum (b) Fluid Lower Plenum (c) Debris Lower Plenum

In the MPS calculation, two input parameters are used: density and kinematic viscosity as the thermophysical properties of a material to distinguish one material from another. The following equations (13) to (19) are used in calculating the density and viscosity for UO_2, ZrO_2, and corium materials as a mixture of UO_2 and ZrO_2 [6],

Density (g/cm^3)

UO_2:
$$\rho(T) = 4.40 - 8.31 \times 10^{-4}(T - 3120) \tag{13}$$

ZrO_2:
$$\rho(T) = 7.56 - 2.86 \times 10^{-4}(T - 2988) \tag{14}$$

Mixture (x: mole fraction):

$$\rho(T) = \frac{x_{UO_2} M_{UO_2} + (1 - x_{UO_2}) M_{ZrO_2}}{x_{UO_2} M_{UO_2}/\rho_{UO_2} + (1 - x_{UO_2}) M_{ZrO_2}/\rho_{ZrO_2}}$$

(15)

Dynamic Viscosity (mPa.s)

UO_2:

$$\mu(T) = 0.520 \times e^{8.26 \times 10^3 / T}$$

(16)

ZrO_2:

$$\mu(T) = 0.320 \times e^{8.79 \times 10^3 / T}$$

(17)

Mixture (x: mole fraction):

$$\ln \mu(T) = x_{UO_2} \ln \mu_{UO_2}(T) + \left(1 - x_{UO_2}\right) \ln \mu_{ZrO_2}(T)$$

(18)

Kinematic Viscosity (m^2/s)

$$\nu = {\mu}/{\rho}$$

(19)

The following shows Table 2, Table 3, Table 4, Table 5, and Table 6 the results of density and viscosity calculations for each material,

Table 2. Density and viscosity of Corium 1

Corium 1 (UO$_2$ 80% & ZrO$_2$ 20%)			
T (Kelvin)	Dynamic Viscosity (Pa.s)	Density (kg/m^3)	Kinematic Viscosity (m^2/s)
3500	0.005151344	4281.091175	1.20328E-06
4000	0.003820846	3864.774559	9.88634E-07
4500	0.003028547	3444.971434	8.79121E-07

Table 3. Density and viscosity of Corium 2

Corium 2 (UO$_2$ 50% & ZrO$_2$ 50%)			
T (Kelvin)	Dynamic Viscosity (Pa.s)	Density (kg/m^3)	Kinematic Viscosity (m^2/s)
3500	0.004660086	4753.055801	9.8044E-07
4000	0.003436899	4342.855324	7.91392E-07
4500	0.002712211	3921.065561	6.91702E-07

Table 4. Density and viscosity of Corium 3

Corium 3 (UO_2 20% & ZrO_2 80%)			
T (Kelvin)	Dynamic Viscosity (Pa.s)	Density (kg/m³)	Kinematic Viscosity (m²/s)
3500	0.004215677	5753.52096	7.32713E-07
4000	0.003091534	5395.621367	5.72971E-07
4500	0.002428916	5014.034478	4.84423E-07

Table 5. Density and viscosity of UO_2

UO_2			
T (Kelvin)	Dynamic Viscosity (Pa.s)	Density (kg/m³)	Kinematic Viscosity (m²/s)
3500	0.005507295	4084.22	1.34843E-06
4000	0.004100355	3668.72	1.11765E-06
4500	0.00325968	3253.22	1.00199E-06

Table 6. Density and Viscosity of ZrO_2

ZrO_2			
T (Kelvin)	Dynamic Viscosity (Pa.s)	Density (kg/m³)	Kinematic Viscosity (m²/s)
3500	0.003943207	7413.568	5.31891E-07
4000	0.002880793	7270.568	3.96227E-07
4500	0.00225669	7127.568	3.16614E-07

After MPS calculation, data processing and simulation are then carried out with ParaView 5.10.1, and graphs are displayed with Microsoft Excel 2016.

In order to carry out characteristic analysis several parameter surveys were carried out to review the characteristics of one parameter against other parameters by varying the parameters reviewed while other parameters were kept constant. Therefore, the sampling method is carried out first by evaluated velocity versus time graphs with constant temperature & lower plenum conditions (4000K & Empty Lower Plenum) for variations of 5 materials. Second, evaluated velocity versus time graphs with material & constant lower plenum conditions (Corium 1 & Empty

Lower Plenum) for 3 temperature variations. Third, evaluated velocity versus time graphs with constant temperature & material (4000K & Corium 1) for variations of 3 lower plenum conditions. Then, evaluated the velocity profile with constant temperature & material (4000K & Corium 1) for 3 variations of lower plenum conditions.

Results and Discussion

Several parameter surveys were carried out by reviewing the velocity versus time graphs, as well as their profiles for various variations of lower plenum conditions as follows,

Parameter Survey I: Material Variation, 4000K, & Empty

Figure 3 shows the graph of velocity versus time with various material corium 1 (80% UO_2 & 20% ZrO_2), corium 2 (50% UO_2 & 50% ZrO_2), corium 3 (20% UO_2 & 80% ZrO_2), UO_2, and ZrO_2 when relocating to an empty lower plenum and a temperature of 4000K. It can be seen that at 30 s as soon as the particles touch the lower plenum, corium particles have a higher velocity than UO_2 and ZrO_2 particles. Along with increasing the composition of ZrO_2 in the corium, the speed of the particles is getting higher when heading to the lower plenum. This happens because as the composition of ZrO_2 in the corium increases, the density of the corium material also increases. It can be seen that the corium 3 material particles have the highest velocity compared to other materials.
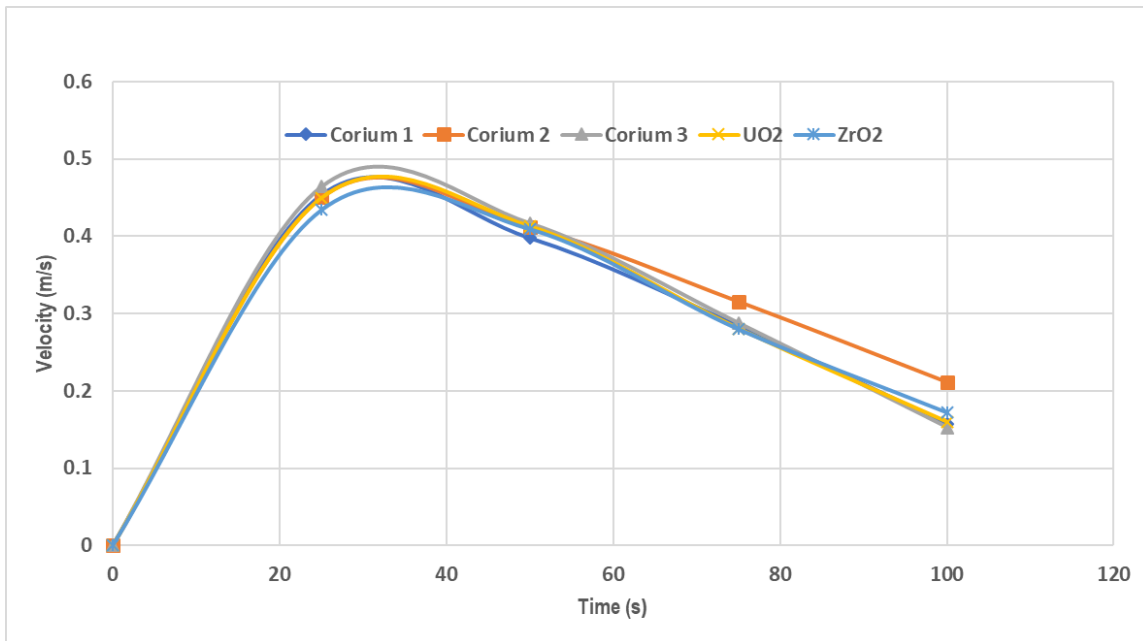
Figure 3.   Graph of velocity-time variations of 5 materials

Parameter II Survey: Temperature Variation, Corium 1, & Empty
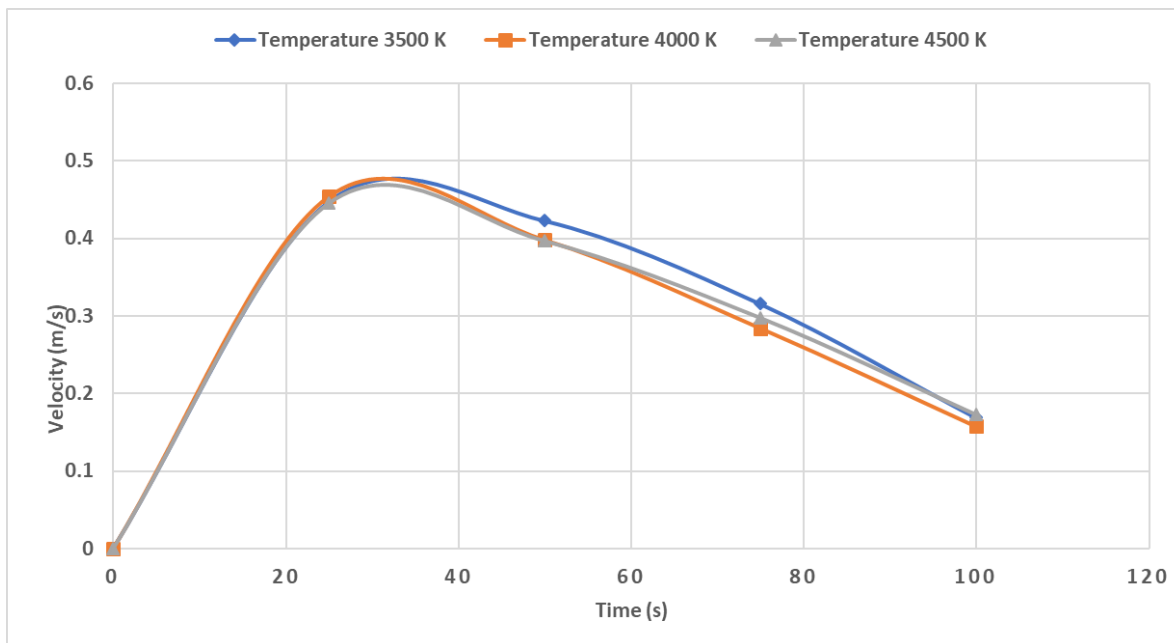
Figure 4.   Graph of velocity-time variations of 5 temperatures

Figure 4 shows the velocity versus time graph with temperature variations of 3500K, 4000K, and 4500K for corium 1 material (80% UO_2 & 20% ZrO_2) and empty lower plenum conditions. It can be seen that at 30 s for a moment the particles touch the lower plenum, the higher the temperature of the material, the lower the velocity of the particles as they go to the lower plenum. This is due to the selection of temperature variations carried out in this study in the range of 3500K– 4500K which is close to the boiling point of the material so that it is possible that some of the particles have changed phase. This is because the study wants to review the characteristics when melting of corium occurs, so the corium temperature is chosen which is close to the average boiling point temperature of the corium material.

Parameter III Survey: Lower Plenum Variation, 4000K, & Corium 1

Figure 5 shows the graph of velocity versus time with variations in lower plenum conditions: empty, fluid, and debris on corium 1 material (80% UO_2 & 20% ZrO_2) and a temperature of 4000K. It can be seen that at 30 s for a moment the particles touch the lower plenum, material particles that have the highest velocity, namely when the condition is empty in the lower plenum, followed by the condition when the debris is in the lower plenum, and when the fluid is in the lower plenum. This is due to the condition of the empty lower plenum, the collision of particles occurs on the lower wall of the lower plenum. Whereas in the lower plenum debris, particle collisions occur on debris particles. Meanwhile in the lower plenum fluid, particle collisions occur on fluid particles, that have the same viscosity value so that they are effective in reducing the particle velocity.
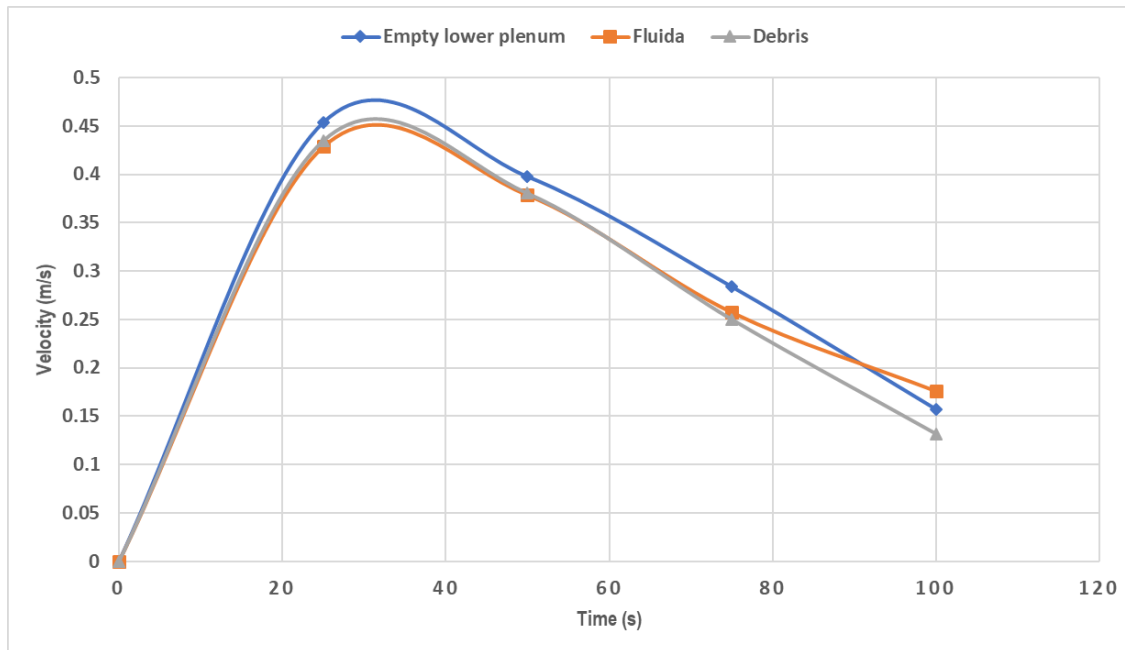
Figure 5. Graph of velocity-time variations of 5 plenums

Velocity Profile: Plenum Variation, 4000K, & Corium 1

Figure 6 is a velocity profile at various conditions of the lower plenum: empty, fluid, and debris in corium 1 material and a temperature of 4000K at a time of 0 s, 25 s, 50 s, 75 s, up to 100 s shown with ParaView 5.10.1. At the time of 25 s, the speed of the particles is very high because the particles are falling towards the lower plenum. Then at 50 s and so on, some of the particles have filled the lower plenum and the speed of the particles decreases along with collisions with other particles due to the formation of a corium pool which can cause several unpredictable possibilities, including the formation of several metal and oxide layers. In the various layers that are formed, the heat flux resulting from the convection process in the corium pool will be different and concentrated in a large part. If the heat flux generated in a part is greater than the critical heat flux that can be compensated by the reactor vessel, then the reactor vessel will experience a decrease in integrity resulting in reactor vessel failure. In addition, at certain compositions, a corium pool can be formed with the bottom layer in the form of heavy metals which can increase the thermal load in the lower plenum [5].

Furthermore, it is likely that debris will form as a result of the corium freezing on contact with water. The formation of debris that accumulates will form a debris bed. Debris formed at high temperatures will cause a significant temperature difference to the reactor vessel wall, so that it can slowly melt the reactor vessel wall. The debris that is formed will be difficult to cool, besides that the debris cooling process can also increase the pressure in the reactor vessel due to water vapor. In addition, debris can also make it difficult to predict the flow of corium to the lower plenum [7].

t = 0 s   t = 25 s   t = 50 s   t = 75 s   t = 100 s

(a)

t = 0 s   t = 25 s   t = 50 s   t = 75 s   t = 100 s

(b)

t = 0 s   t = 25 s   t = 50 s   t = 75 s   t = 100 s

(c)
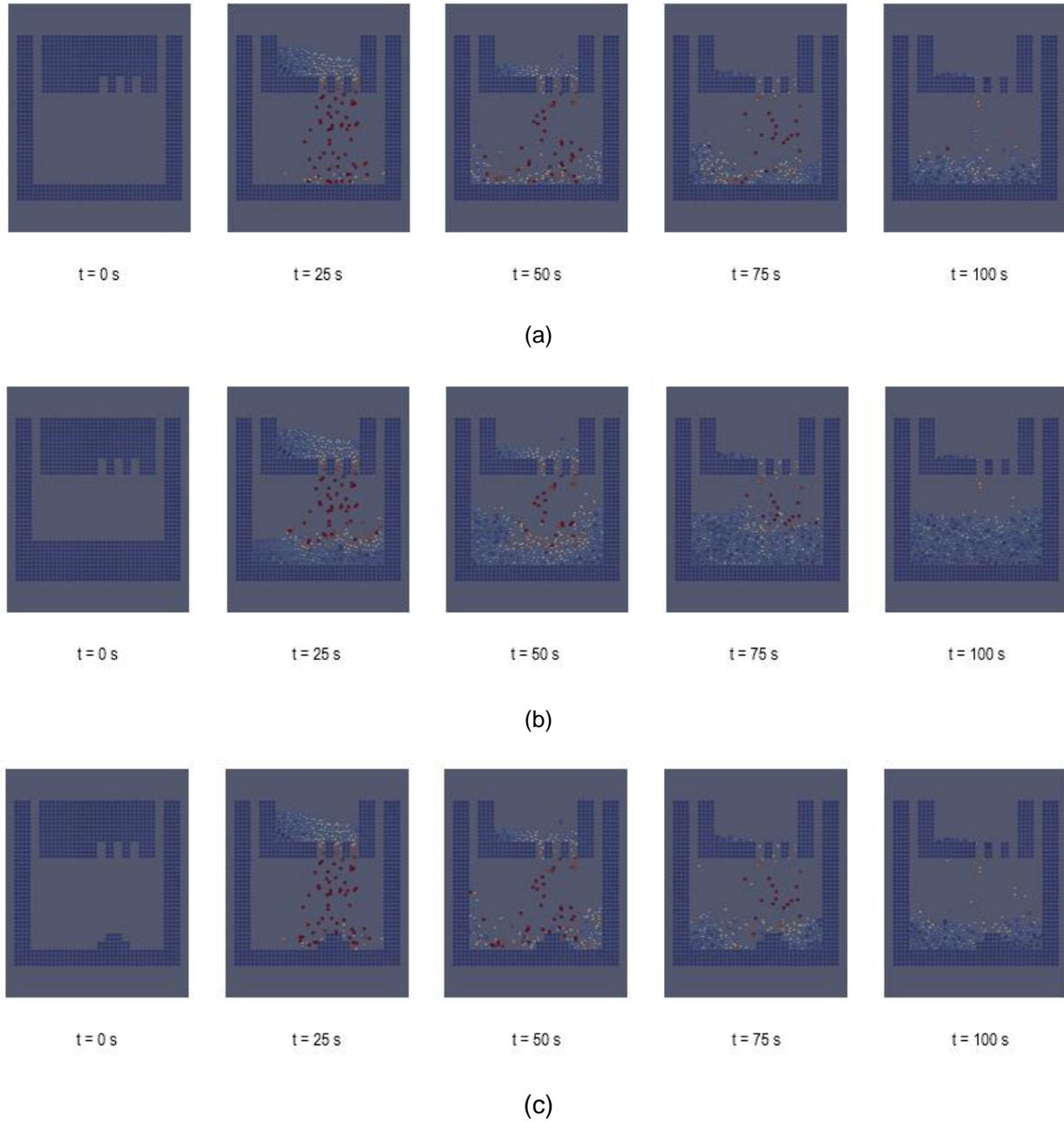
Figure 6.   Velocity profile for variations of lower plenum, 4000K, & Corium 1 (a) empty, (b) fluid, (c) debris

Conclusions

Simulation and analysis of the relocation characteristics of molten corium during the reactor severe accident using the MPS method have been carried out with variations in corium material,

variations in lower plenum conditions, variations in temperature, variations in viscosity, and variations in density with simplification and scale-down of the reactor geometry. From this work, it can be concluded several important results, including: (a) Along with increasing the composition of ZrO_2 in the corium, the speed of the particles is getting higher when heading to the lower plenum. This happens because as the composition of ZrO_2 in the corium increases, the density of the corium material also increases, (b) Ideally, as the temperature increases, the density and viscosity will decrease, causing the particle velocity to decrease. This is due to the selection of temperature variations carried out in the range of 3500K – 4500K which is close to the boiling point of the material so that it is possible that some of the particles have changed phase, (c) Material particles that have the highest velocity is the empty lower plenum condition, followed by the debris lower plenum condition, then the fluid lower plenum condition, (d) The formation of a corium pool and debris bed could cause in significant temperature differences and high heat flux against the walls of the reactor vessel, causing a decrease in the integrity of the reactor vessel and reactor failure, (e) To minimize the occurrence of the system failure for core melting, it can be done by trying to slow down the relocation velocity of the corium particles when melting occurs. This can be done by choosing a corium material with a relatively low ZrO_2 composition, by keeping the operating temperature of the reactor within a safe range to avoid corium melting, corium pool and debris bed formation which can cause significant temperature differences and high heat flux to the the walls of the reactor vessel causing a decrease in the integrity of the reactor vessel and the failure of the reactor.

ACKNOWLEDGEMENTS

References
[1]   A. C. Cilliers, 2013, *Benchmarking an expert fault detection and diagnostic system on the Three Mile Island accident event sequence*, Annals of Nuclear Energy, volume 62, pages 326-332. DOI: 10.1016/j.anucene.2013.06.037.

[2]   S. Koshizuka and Y. Oka, 1996, *Moving-Particle Semi-Implicit Method for Fragmentation of Incompressible Fluid*, Nuclear Science and Engineering, volume 123, pages 421 – 434.

[3]   A. N. Hidayati, A. Waris, A. P. Andi Mustari, N. A. Apriani, M. Ifthacharo and R. Wulandari, 2020, *The Effect of Temperature Variations on Wood's Metal Plate Melting Simulation by Using MPS*, Journal of Physics: Conference Series, volume 1493, no. 1. DOI: 10.1088/1742-6596/1493/1/012024.

[4]   A. Yamaji and X. Li, 2016, *Development of MPS Method for Analyzing Melt Spreading Behavior and MCCI in Severe Accidents*, Journal of Physics: Conference Series, volume 739, no. 1. DOI: 10.1088/1742-6596/739/1/012002.

[5]   L. Liu, H. Yu, J. Deng, L. Chen, C. Deng, Q. Xiang and L. Wu, 2019, *Analysis of the configurations and heat transfer of corium pool in RPV lower plenum,* Annals of Nuclear Energy, volume 124, pages 172–178.

DOI:10.1016/j.anucene.2018.10.002.

[6]   K.K. Woong, J.H. Shim and K. Massoud, 2017, *Thermophysical properties of liquid UO$_2$, ZrO$_2$ and corium by molecular dynamics and predictive models*, Journal of Nuclear Materials, volume 491, pages 126-137,
DOI:10.1016/j.jnucmat.2017.04.030.

[7]   L. Viot, R. Le Tellie and M. Peybernes, 2020, *Modeling of the corium crust of a stratified corium pool during severe accidents in light water reactors*, Nuclear Engineering and Design, volume 368, no.110816,
DOI: 10.1016/j.nucengdes.2020.110816.